Role of the Central Metal Ion and Ligand Charge in the DNA Binding and Modification by Metallosalen Complexes

Subhrangsu S. Mandal,[†] Umesh Varshney,[‡] and Santanu Bhattacharya*[,†]

Department of Organic Chemistry and Center for Genetic Engineering, Indian Institute of Science, Bangalore 560012, India. Received November 14, 1996[⊗]

Several metal complexes of three different functionalized salen derivatives have been synthesized. The salens differ in terms of the electrostatic character and the location of the charges. The interactions of such complexes with DNA were first investigated in detail by UV−vis absorption titrimetry. It appears that the DNA binding by most of these compounds is primarily due to a combination of electrostatic and other modes of interactions. The melting temperatures of DNA in the presence of various metal complexes were higher than that of the pure DNA. The presence of additional charge on the central metal ion core in the complex, however, alters the nature of binding. Bis-cationic salen complexes containing central Ni(II) or Mn(III) were found to induce DNA strand scission, especially in the presence of co-oxidant as revealed by plasmid DNA cleavage assay and also on the basis of the autoradiogram obtained from their respective high-resolution sequencing gels. Modest base selectivity was observed in the DNA cleavage reactions. Comparisons of the linearized and supercoiled forms of DNA in the metal complex-mediated cleavage reactions reveal that the supercoiled forms are more susceptible to DNA scission. Under suitable conditions, the DNA cleavage reactions can be induced either by preformed metal complexes or by *in situ* complexation of the ligand in the presence of the appropriate metal ion. Also revealed was the fact that the analogous complexes containing Cu(II) or Cr(III) did not effect any DNA strand scission under comparable conditions. Salens with pendant negative charges on either side of the precursor salicylaldehyde or ethylenediamine fragments did not bind with DNA. Similarly, metallosalen complexes with net anionic character also failed to induce any DNA modification activities.

INTRODUCTION[1]

Design and synthesis of small synthetic systems that recognize specific sites of DNA is an important area of much current research (*1*). These could be at least in part due to the formation of noncovalently associated complexes by several such molecules with nucleic acids. Many times, such physical complexation may produce important pharmacological effects by interfering with the biological processes in which DNA/RNAs take part. Such investigations also sometimes provide insights for the mechanism of action of naturally occurring antitumor antibiotics (*2*). Toward this direction, there is a continuing search for new metal complexes that strongly interact with DNA. These studies led to the development of several new reagents. Examples include complexes *e.g.* iron−EDTA (*3*), copper− or rhodium−1,10-phenanthroline (*4*, *5*), manganese−porphyrin (*6*), platinum−diamine (*7*), nickel−cyclam (*8*), and several photonucleases (*9*), among others. Examination of the interactions of transition metal complexes with DNA aids in the development of new reagents that are potentially useful in molecular biology (*10*) and also in the design of putative drugs (*11*). Utilities of some metal complexes as structural probes (*1*, *12*) for DNA and in drug/protein−DNA footprinting (*10*, *13*) are also known. Sometimes, such studies also offer useful leads in the elucidation of potential toxicities of various metal complex-based systems (*14*).

Earlier investigations (*16*−*19*) have indicated that, while some metallosalen derivatives bind DNA avidly (*15*), few others induce effective DNA scission (*16*−*19*) or inhibit lymphocyte proliferation (*20*). Therefore, subtle variation in the structure of the salen unit and variation of the central metal ion influence the effect of the resulting complex on DNA in a widely unrelated fashion. Griffin carefully studied (*16*) some of these aspects of DNA modification in detail with manganese−salen complexes. Burrows and Rokita synthesized (*17*) some nickel−salen derivatives which induced DNA cross-linking. More recently, Routier *et al*. examined the interaction of DNA with a functionalized salen−copper-(II) complex which induced DNA strand scission in the presence of a reducing agent (*18*). We also examined the DNA cleavage processes induced by some bis-cationic salen analogues (*19*). Examination of the above reports makes it clear that much still remains to be understood about the role of salen structure and that of the central metal ion in the DNA binding/modification processes. We thought that a progressive structural variation of the salens with respect to charge on the aryl rings, at the imine portions, and systematic variation of the central metal ion under a given ligand (salen) environment might provide additional insight on the factors involved in the chemistry of binding and DNA modification by such complexes. Herein, we report the synthesis of a number of transition metal complexes based on a few different water-soluble salen derivatives, **1**−**5**. The results of the binding abilities of different metal complexes with native *Escherichia coli* genomic DNA at various salt concentrations and with alkali-denatured DNA and the effects of such binding on DNA melting are included in this report.

* To whom correspondence should be addressed. Also at Chemical Biology Unit, Jawaharlal Nehru Centre for Advanced Scientific Research, Bangalore 560064, India.
[†] Department of Organic Chemistry.
[‡] Center for Genetic Engineering.
[⊗] Abstract published in *Advance ACS Abstracts,* August 1, 1997.
[1] **Caution**. Although we did not experience any difficulty while working with these systems, perchlorate salts are potentially explosive!

S1043-1802(97)00121-3 CCC: $14.00

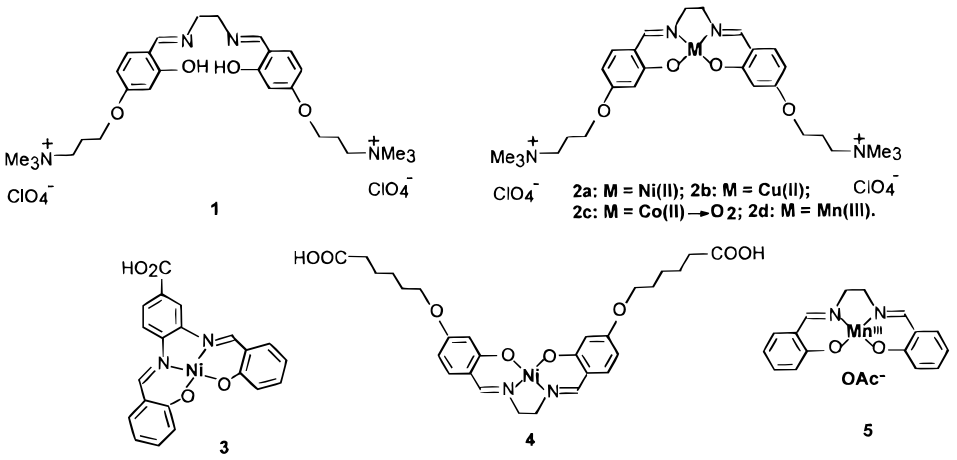

The DNA cleavage reactions and the nicking patterns produced by different metal complexes are also presented.

EXPERIMENTAL PROCEDURES

General Aspects. Melting points were determined in open capillaries and are uncorrected. Infrared spectra were recorded with a Shimadzu FTIR 8101 infrared spectrophotometer equipped with a DR-8001 workstation. ^{1}H-NMR spectra were recorded with a Bruker AC-200 (200 MHz) or a Jeol FX-90 (90 MHz) NMR spectrometer using $CDCl_3$ or the appropriate deuterated solvent. Elemental analyses were performed by the microanalytical division of the Department of Organic Chemistry at the Indian Institute of Science in Bangalore and were run on a Carlo Erba model 1106 elemental analyzer. These are presented as percents. Electronic spectra were recorded on a Shimadzu model 2100 UV−visible spectrophotometer equipped with a TCC-60 temperature controller unit or a Julabo F-10 water-circulating temperature-controlled bath.

Materials. Silica gel (UV_{254}) plates (Sigma) were used for TLC. Column chromatography was performed on silica gel (60−120 mesh) from Merck (Schuchardt, Germany). Commercial compounds used in the synthesis and other studies herein were purchased from best known suppliers and used as received; solvents were purified and dried by standard methods. All other materials used for preparing buffers were of the highest quality commercially available. Millipore grade water was used for all the experiments. The enzymes used in this study were obtained from Pharmacia.

Calf thymus DNA (CT DNA) obtained from Sigma Chemical Co. (St. Louis, MO) was purified by phenol−chloroform extraction followed by ethanol precipitation as described previously (*21*). Solutions of CT DNA in 10 mM Tris-HCl, 1 mM EDTA buffer (pH 7.4) gave a ratio of the UV absorbances at 260 and 280 nm (A_{260}/A_{280}) of >1.9. The DNA concentrations were determined by using an extinction coefficient of 6600 M^{-1} cm^{-1} at 260 nm and were expressed in terms of base molarity (*22*). Melting temperature determinations and the spectroscopic binding studies were performed with CT DNA in 10 mM Tris-HCl, 1 mM EDTA buffer (pH 7.4).

E. coli genomic DNA was isolated and purified as described (*23*). Briefly, *E. coli* cells (CA 274 strain) were overgrown in LB media, and the cells were subjected to lysozyme treatment, followed by lysis with SDS and proteinase K treatment. The mixture was finally subjected to phenol−chloroform extraction two times, and the DNA was precipitated using 2-propanol and washed with 70% ethanol. Then, the DNA was dissolved in 10 mM Tris-HCl, 1 mM EDTA buffer (pH 7.4) which gave an A_{260}/A_{280} of ∼1.9.

The plasmid DNA pTZ19R used herein was grown in *E. coli* cells and isolated in our laboratory as described earlier (*19a*). The supercoiled plasmid was obtained by CsCl/ethidium bromide density gradient centrifugation.

Synthetic Methods. *4-[(3-Bromopropyl)oxy]salicylaldehyde (6).* A mixture of 138 mg (1 mmol) of 2,4-dihydroxybenzaldehyde and 404 mg (2 mmol) of 1,3-dibromopropane was refluxed in the presence of 140 mg (1.4 mmol) of $KHCO_3$ in 50 mL of dry acetone for 60 h. At the end of this period, the solvent from the reaction mixture was removed in a rotavapor, 5 mL of water was added to it, and then the solvent was extracted with 3 × 10 mL portions of $CHCl_3$. The combined chloroform extracts were evaporated to dryness and then purified by column chromatography over silica gel (60−120 mesh) using 2−3% EtOAc in light petroleum (60−80 °C boiling fraction). Upon chromatographic purification, a white crystalline solid was obtained in *ca.* 60% yield: mp 62−64 °C; ^{1}H-NMR (200 MHz, $CDCl_3$) δ 2.3 (2H, m, CH_2CH_2-CH_2Br), 3.6 (2H, t, CH_2Br), 4.2 (2H, t, CH_2CH_2O), 6.45 (1H, d, ArH_3, J_m = 2.0 Hz), 6.55 (1H, dd, ArH_5, J_m = 2 Hz, J = 9.5 Hz), 7.5 (1H, d, ArH_6, J_0 = 9.5 Hz), 9.7 (1H, s, C*H*O), 11.5 (1H, s, ArO*H*); IR (Nujol) (cm^{-1}) 1630 (s), 1510, 1210, 1095. Anal. Calcd for $C_{10}H_{11}BrO_3$: C, 46.35; H, 4.27. Found: C, 46.42; H, 4.26.

4-[[3-(Trimethylammonio)propyl]oxy]salicylaldehyde Bromide (6a). One hundred milligrams (0.38 mmol) of **6** was dissolved in 20 mL of EtOAc in a screw-top pressure tube. Two milliliters of dry trimethylamine gas was passed into this solution precooled at ∼0−5 °C. Then, the screw top of the tube was closed tightly and the tube allowed to stand for 6 h at ambient temperature. At the end of this period, a brownish-white solid was obtained. The solid was collected by filtration and was recrystallized from a mixture of EtOAc/EtOH. Recrystallization afforded a colorless, crystalline, hygroscopic product in practically quantitative yield: mp 152−154 °C; ^{1}H-NMR (90 MHz, D_2O) δ 2.4 (2H, m, $CH_2CH_2CH_2N^+Me_3$), 3.2 (9H, s, N^+-$(CH_3)_3$), 3.6 (2H, t, $CH_2N^+Me_3$), 4.23 (2H, t, ArOCH_2), 6.52 (1H, d, ArH_3, J_m = 2.0 Hz), 6.68 (1H, dd, ArH_5, J_m = 2 Hz, J = 9.5 Hz), 7.68 (1H, d, ArH_6, J_0 = 9.5 Hz), 9.8 (1H, s, C*H*O); IR (Nujol) (cm^{-1}) 1630 (s), 3400 (s). Anal. Calcd for $C_{13}H_{20}NO_3Br\cdot H_2O$: C, 46.44; H, 6.59; N, 4.17. Found: C, 46.41; H, 6.30; N, 4.02.

4-[[3-(Trimethylammonio)propyl]oxy]salicylaldehyde Perchlorate (6b). The above material, 4-[[3-(trimethylammonio)propyl]oxy]salicylaldehyde bromide (**6a**, 425 mg, 1.3 mmol), was dissolved in 1 mL of water, and the resulting aqueous solution was treated with 1 mL of aqueous $NaClO_4$ (327 mg, 2.6 mmol). This resulted in

the formation of the corresponding perchlorate salt which precipitated as a white solid. This was filtered and dried in a desiccator, *ca*. 95% yield: mp 140−142 °C; ^{1}H-NMR (200 MHz, DMSO-d_6) δ 2.1 (2H, m, $CH_2CH_2CH_2N^+Me_3$), 3.05 (9H, s, $N^+(CH_3)_3$), 3.4 (2H, t, $CH_2N^+Me_3$), 4.05 (2H, t, $ArOCH_2$), 6.3 (1H, d, ArH_3), 6.5 (1H, dd, ArH_5), 7.5 (1H, ArH_6, d), 9.5 (1H, s, CHO); IR (Nujol) (cm^{-1}) 1630 (s), 1460 (s), 1375 (s), 1230 (s), 1100 (s), 625 (s). Anal. Calcd for $C_{13}H_{20}NO_7Cl$: C, 46.23; H, 5.97; N, 4.15. Found: C, 46.21; H, 6.01; N, 4.02.

N,N′-Bis[4-[[3-(trimethylammonio)propyl]oxy]salicylidene]ethylenediamine Diperchlorate (1). **6b**, 4-[[3-(trimethylammonio)propyl]oxy]salicylaldehyde perchlorate (250 mg, 0.74 mmol), was dissolved in 10 mL of dry MeOH by careful warming. To this was added 22.2 mg (0.37 mmol) of freshly distilled ethylenediamine, and the resulting mixture was warmed to ∼60 °C for 10 min which upon cooling to ambient temperature produced a yellow precipitate. The yellow residue was isolated and washed with cold MeOH and dried (yield *ca*. 80%): mp 258−260 °C; ^{1}H-NMR (90 MHz, DMSO-d_6) δ 2.1 (4H, m, $CH_2CH_2CH_2NMe_3$), 3.05 (18H, s, $N(CH_3)_3$), 3.4 (4H, t, CH_2NMe_3), 3.9 (4H, s, $=NCH_2CH_2N=$), 4.05 (4H, t, $ArOCH_2$), 6.3−6.45 (4H, m, ArH_3, ArH_5), 7.2 (2H, d, ArH_6), 8.45 (2H, s, ArHC=N); IR (Nujol) (cm^{-1}) 1630 (s), 1610 (s), 1520 (s), 1460 (s), 1370 (s), 1210 (s), 1095 (s), 620 (s). Anal. Calcd for $C_{28}H_{44}N_4O_{12}Cl_2$: C, 48.06; H, 6.34; N, 8.0. Found: C, 47.62; H, 6.33; N, 7.90.

N,N′-Bis[4-[[3-(trimethylammonio)propyl]oxy]salicylidene]ethylenediamine−Nickel (II) Bisperchlorate (2a). **1** (55 mg, 0.079 mmol) was suspended in 10 mL of dry MeOH. $NiCl_2{\cdot}6H_2O$ (15 mg, 0.08 mmol) was added in the form a methanolic solution into this suspension, and the resulting mixture was warmed at 60 °C for 30 min. This gave a deep-red solution which was first allowed to cool to room temperature and then kept in a refrigerator for 48 h. A red-colored, hygroscopic, crystalline precipitate separated out which was collected after filtration, recrystallized from dry MeOH, and dried (yield *ca*. 42%): UV−vis [λ_{max} (nm), ϵ] 1:1 (CH_3CN/CH_3OH) 348 (25 000), 304 (29 000), 236 (14 000), 211 (20 000); IR (KBr pellet) (cm^{-1}) 600 (m), 730 (m), 920 (m), 1040 (m), 1120 (s), 1200 (s), 1215 (s), 1300 (m), 1420 (m), 1480 (s), 1490 (s), 1530 (s), 1600 (s). Anal. Calcd for $C_{28}H_{42}N_4O_{12}Cl_2Ni{\cdot}2.5H_2O$: C, 41.94; H, 5.28; N, 6.99. Found: C, 42.01; H, 5.49; N, 6.99.

N,N′-Bis[4-[[3-(trimethylammonio)propyl]oxy]salicylidene]ethylenediamine−Copper(II) Bisperchlorate (2b). The ligand **1** (40 mg, 0.05 mmol) was suspended in 10 mL of dry MeOH, to which a methanolic solution of 16 mg (0.08 mmol) of $Cu(OAc)_2{\cdot}4H_2O$ was added, and the resulting mixture was warmed for 30 min at 60 °C. The solution slowly turned into a bluish pink color which upon cooling gave a pink crystalline precipitate. The residue was collected by filtration and repeatedly recrystallized from dry MeOH to give a pink hygroscopic solid (yield *ca*. 60%): UV−vis [λ_{max} (nm), ϵ] (H_2O) 365.5 (10 000), 282.5 (20 000), 249.5 (30 000), 226 (29 000); IR (KBr pellet) (cm^{-1}) 620 (s), 840 (m), 1090 (s), 1110 (s), 1210 (s), 1400 (m), 1540 (m), 1610 (s). Anal. Calcd for $C_{28}H_{42}N_4O_{12}CuCl_2{\cdot}1H_2O$: C, 43.10; H, 5.43; N, 7.18. Found: C, 42.89; H, 5.54; N, 7.08. EPR: A_{II} 190.1 G, g_{II} 2.2.

N,N′-Bis[4-[[3-(trimethylammonio)propyl]oxy]salicylidene]ethylenediamine−Cobalt(II) Bisperchlorate as a Monomeric Oxygen Adduct (2c). **1** (30 mg, 0.043 mmol) was suspended in 10 mL of dry MeOH. To this was added a methanolic solution of 17.5 mg (0.07 mmol) of $Co(OAc)_2{\cdot}4H_2O$, and the resulting mixture was warmed at 60 °C for 30 min. This gave a brownish-red solution which gradually changed into a deep dark brown color upon standing at ambient temperature in exposure to air. It was kept for 1 week in this manner, from which a dark brown complex was precipitated upon addition of dry ether (yield *ca*. 44%): UV−vis [λ_{max} (nm), ϵ] (H_2O) 361 (7100), 289 (broad hump), 258 (48 000); FTIR (KBr pellet) (cm^{-1}) 625 (s), 940 (m), 1000 (w), 1090 (s), 1125 (s), 1145 (s), 1200 (m), 1430 (s), 1550 (s), 1600 (s), 1620 (s). Anal. Calcd for $C_{28}H_{42}N_4O_{12}CoCl_2O_2{\cdot}2H_2O$: C, 40.97; H, 5.62; N, 6.79. Found: C, 40.94; H, 5.63; N, 6.35 (*24*).

N,N′-Bis[4-[[3-(trimethylammonio)propyl]oxy]salicylidene]ethylenediamine−Manganese(III) Trisperchlorate (*2d*). The ligand **1** (66 mg, 0.09 mmol) was suspended in 15 mL of dry MeOH to which was added a methanolic solution of 26.7 mg (0.2 mmol) of $Mn(OAc)_3{\cdot}4H_2O$ and heated at 60 °C for 30 min. The initial yellowish color of the solution of the Schiff base soon changed into a grayish-black solution from which 70% of the MeOH was removed under vacuum. Upon addition of dry ether to this, a grayish-black solid separates out followed by cooling in a refrigerator. The solid was repeatedly recrystallized from dry MeOH to give a hygroscopic material of 44% yield: UV−vis [λ_{max} (nm), ϵ] (CH_3CN) 343 (15 400), 303 (21 400), 237 (12 300), 208 (17 400); FTIR (KBr pellet) (cm^{-1} 630 (s), 850 (w), 1000 (w), 1095 (s), 1110 (s), 1150 (s), 1300 (w), 1400 (w), 1490 (w), 1530 (w), 1600 (s). Anal. Calcd for $C_{28}H_{42}N_4O_{16}Cl_3Mn{\cdot}2.5H_2O$: C, 37.49; H, 5.28; N, 6.24. Found: C, 37.32; H, 5.17; N, 6.15.

N,N′-Bis(salicylidene)-3,4-diaminobenzoic Acid−Nickel(II) (3). To a solution of 400 mg (3.3 mmol) of salicylaldehyde in 10 mL of MeOH was added with stirring a methanolic solution of 250 mg (1.6 mmol) of freshly recrystallized 3,4-diaminobenzoic acid. From this solution after some time, an orange-colored crystalline solid precipitated out, which was filtered, dried, and then recrystallized from MeOH. This orange Schiff base (100 mg) was dissolved in hot MeOH; to this was added a methanolic solution of 46.7 mg (0.28 mmol) of the $NiCl_2$, and the resulting mixture was heated at 60 °C for 30 min. This produced a transparent deep red-colored solution which upon on standing at ambient temperature gave an orange-red-colored precipitate which was filtered and recrystallized from a mixture of MeOH and $CHCl_3$ in 80% yield. Anal. Calcd for $C_{21}H_{14}N_2O_4Ni{\cdot}0.5CHCl_3$: C, 53.16; H, 3.22; N, 5.76. Found: C, 53.38; H, 3.45; N, 6.05.

[(6-Oxo-6-ethoxyhexyl)oxy]benzaldehyde (7). A mixture of 1.198 g (8 mmol) of 2,4-dihydroxybenzaldehyde and 2 g of ethyl 6-bromohexanoate was refluxed in dry acetone for 2 days in the presence of 800 mg (8 mmol) of anhydrous $KHCO_3$. Then, the solvent form this reaction mixture was removed, and 5 mL of water was added into the residue. The resulting mixture was extracted with 3 × 30 mL of chloroform. The chloroform extract was evaporated to dryness and then purified by column chromatography over silica gel (60−120 mesh) using 2% EtOAc in light petroleum (60−80 °C boiling fraction). Upon concentration of the eluted fraction, a highly viscous liquid was obtained in *ca*. 50% yield: IR (neat) (cm^{-1}) 3250−3400 (br), 2900 (s), 1715 (s), 1620 (s), 1495 (s), 1200 (s), 1100 (s), 1000 (s); ^{1}H-NMR (90 MHz, $CDCl_3$) δ 1.2 (3H, t, CH_2CH_3), 1.5−2.0 (6H, m, $OCH_2(CH_2)_3CH_2$), 2.4 (2H, t, CH_2COO), 4.05−4.2 (4H, m, $ArOCH_2$, + $COOCH_2CH_3$), 6.45 (1H, d, ArH_3, $J_m \sim 1.5$ Hz), 6.55 (1H, dd, ArH_5, $J_m \sim 1.5$ Hz, $J_0 \sim 9.4$ Hz), 7.4 (1H, d, ArH_6, $J_o \sim 9.4$ Hz), 9.8 (1H, s, CHO), 11.5 (1H, s, ArOH).

[(6-Hydroxy-6-oxohexyl)oxy]benzaldehyde (7a). Compound **7** was saponified under refluxing conditions using 2% aqueous NaOH. The resulting reaction mixture was cooled in ice and neutralized by dropwise addition of concentrated HCl under ice-cold conditions. This gave

a white precipitate which was filtered, and the residue was washed with cold water, dried, and then purified by column chromatography over silica gel (60−120 mesh) using 2% MeOH in $CHCl_3$. The purified material was recrystallized from EtOAc to afford a solid in 80% yield: mp 124−125 °C; IR (Nujol) (cm^{-1}) 3320 (s), 1710 (s), 1610 (s), 1460 (s), 1370 (s), 1300 (s), 1200 (s), 1050 (s), 860 (s); ^{1}H-NMR (90 MHz, $CDCl_3$) δ 1.8 (6H, m, $OCH_2(CH_2)_3CH_2$), 2.2 (2H, t, CH_2COO), 4.0 (2H, t, $ArOCH_2$), 6.45 (1H, d, ArH_3, $J_m \sim 1.5$ Hz), 6.6 (1H, dd, ArH_5, $J_m = 1.5$ Hz, $J_o \sim 9.4$ Hz), 7.3 (1H, d, ArH_6, $J_o \sim 9.4$ Hz), 9.8 (1H, s, CHO), 11.45 (1H, s, ArOH). Anal. Calcd for $C_{13}H_{16}O_5$, 0.4-EtOAc: C, 62.38; H, 6.83. Found: C, 62.71; H, 6.83.

N,N′-Bis[4-[(6-hydroxy-6-oxohexyl)oxy]salicylidene]Ethylenediamine−Nickel(II) (4). **7a** (252 mg, 1 mmol) was suspended in 5 mL of dry MeOH. Freshly distilled ethylenediamine (30 mg, 0.5 mmol) was added into this. The resulting yellowing solution was stirred and warmed for 5 min which on prolonged standing at ambient temperature gave a yellow-colored precipitate, **7b**. This was filtered, washed with cold MeOH, and dried (yield of 90%). The Schiff base **7b** (100 mg, 0.18 mmol) was suspended in 5 mL of a mixture of dry MeOH and $CHCl_3$. A methanolic solution containing 31 mg (0.18 mmol) of $NiCl_2$ was added to this, and the mixture was warmed for 30 min at 60 °C. During warming, the yellow suspension got slowly converted to a deep red solution which on cooling and standing at ambient temperature for several hours gave a red-colored crystalline precipitate. It was filtered, and the residue was washed with ice-cold, dry MeOH and then recrystallized from a mixture of MeOH and $CHCl_3$ to yield a material of *ca.* 70% yield: UV−vis [λ_{max} (nm), ϵ] [5 mM Tris-HCl buffer (pH 7.4) 376 (7000), 258 (41 000); FTIR (KBr pellet) (cm^{-1}) 700 (s), 760 (w), 800 (w), 830 (m), 1110 (s), 1200 (s), 1220 (s), 1540 (s), 1600 (s), 1700 (s). Anal. Calcd for $C_{28}H_{34}N_2O_8Ni \cdot 0.75CHCl_3$: C, 51.17; H, 5.19; N, 4.15: Found: C, 50.84; H, 5.30; N, 4.37.

N,N′-Bis(salicylidene)ethylenediamine−Manganese-(III) Acetate (5). This was prepared by following a literature procedure (*16a*). Briefly, 569 mg (2.1 mmol) of *N,N′*-bis(salicylidene)ethylenediamine was dissolved in 10 mL of dry MeOH, to which was added a methanolic solution of 442 mg (2.2 mmol) of $Mn(OAc)_3 \cdot 4H_2O$, and the resulting mixture was warmed at 60 °C for 30 min. Then, it was allowed to cool to room temperature. Upon addition of dry ether to this, a gray-black precipitate was obtained. This compound showed all the properties as reported previously (*16a*) (yield of 70%): IR (cm^{-1}) 1630 (s), 1595 (s), 1560 (s), 1460 (s), 1440 (s), 1385 (s), 1330 (s), 1290 (s), 1200 (m), 1140 (m), 1130 (s), 1080 (m), 1030 (m), 960 (m), 900 (s), 800 (s), 770 (s); UV−vis [λ_{max} (nm), ϵ] (ethanol) 400 (6100), 350 (8000), 310 (16 000), 283 (21 000), 220 (41 000). Anal. Calcd for $C_{18}H_{17}N_2O_4Mn$: C, 56.85; H, 4.50; N, 7.37. Found: C, 56.82; H, 4.47; N, 7.11.

Absorption Titration. Absorption titrations were carried out by keeping the concentration of the probe constant while adding a concentrated solution of the *E. coli* genomic DNA in 1 mM Tris-HCl, 0.1 mM EDTA buffer (pH 7.4) in increasing amounts in both the cuvettes until the saturations in hypochromism were observed. The saturation in hypochromism is quantitatively shown by plotting the A_0/A *vs* [DNA], where A_0 and A are the absorption intensities of the individual metal complexes in the absence and presence of various concentrations of DNA, respectively. The intrinsic binding constants for the different metal complexes with DNA were determined by the half-reciprocal plot method as given in the literature (*25*). The intrinsic binding constant (K) for a given complex with DNA was then obtained from a plot of $D/\Delta\epsilon_{ap}$ *vs* D according to eq 1, $D/\Delta\epsilon_{ap} = D/\Delta\epsilon + 1/(\Delta\epsilon K)$ (1) where D is the concentration of DNA in base molarity, $\Delta\epsilon_{ap} = |\epsilon_a - \epsilon_f|$, and $\Delta\epsilon = |\epsilon_b - \epsilon_f|$, where ϵ_b and ϵ_f are respective extinction coefficients of the complex in the presence and absence of DNA, respectively. The apparent extinction coefficient, ϵ_a, was obtained by calculating A_{obsd}/[complex]. The data were fitted to eq 1, with a slope equal to $1/\Delta\epsilon$ and a y-intercept equal to $1/(\Delta\epsilon K)$. The intrinsic binding constants (K) were determined from the ratio of the slope to the y-intercept.

Effect of the Addition of Salt on DNA Binding. To find out the effect of the variation in the ionic strength on the binding abilities of metal complexes with CT DNA, we studied the effects of addition of various salts to a solution containing DNA−**2b** complexes by adding increasing amounts of different salt solutions (30 and 45 mM NaCl or 15 mM $MgCl_2$) to the **2b**−DNA complex. The effects of such additions were followed by UV−vis absorption spectroscopy (*26*).

DNA Denaturation and Binding of Metallosalen. The comparative binding efficiencies of the Ni complex (**2a**) toward double-stranded and alkali-denatured CT DNA were studied by using UV−vis absorption spectroscopy. The denatured CT DNA was obtained by incubating the DNA in 1 M NaOH at room temperature for 10 min. The spectrum of the Ni complex (**2a**) was recorded first; then, 5 μL of alkali-denatured CT DNA was added to this, and the changes in the spectra were then recorded again. The pH of the resulting solution was then slowly decreased by the addition of increasing amounts of HCl until the saturation in binding was reached.

Melting Temperatures. Melting temperatures for DNA in the absence and in the presence of various metal complexes were measured by following the changes in the UV−vis absorption spectra at 260 nm as a function of temperature in a Shimadzu model UV-2100 UV−vis spectrophotometer. The absorption intensities at 260 nm were plotted against individual temperatures in the presence of each metal complex, and the midpoints of the inflection regions in the temperature *vs* A_{260} curves were taken as the corresponding T_m values (*27*). The temperatures of the cuvettes were maintained using a Julabo model F-10 water-circulating bath. Each melting temperature determination employed 72 μM (base molarity) CT DNA in 5 mM Tris-HCl buffer (pH 7.4).

DNA Cleavage Experiments. The DNA cleavage or modification reactions induced by different metal complexes in the absence and in the presence of co-oxidants were performed using the supercoiled plasmid pTZ19R (2.9 kbp, Pharmacia) in 20 mM Tris-HCl buffer (pH 7.4). In a typical experiment, the plasmid DNA (0.25 μg/reaction) was incubated in a reaction mixture (10 μL) containing various concentrations of individual metal complexes (either preisolated or prepared *in situ*) in 20 mM Tris-HCl buffer (pH 7.4) at 37 °C. Reactions were initiated by the addition of MMPP (0.5 mM) and were stopped after 5 min by the addition of a terminating agent (5 μL) containing 10 mM β-mercaptoethanol, 20% glycerol, 25 mM EDTA, and 0.05% bromophenol blue/xylene cyanol (1:1). Then, this was kept on ice. The samples were loaded on 1% neutral agarose gel and were subjected to electrophoresis in a horizontal slab gel apparatus using 0.5 × TBE as the buffer (at 100 V for ∼ 1.5 h). After electrophoresis, the gels were stained with a solution of 0.5 μg/mL ethidium bromide for ∼60 min and then destained. Bands of DNA were then visualized under UV light (photodyne transilluminator, 312 nm) and photographed (Canon SLR camera with an orange filter) in a darkroom.

Sequencing and Autoradiogram. The sequence or base selectivities in the DNA modification reactions effected by different salen complexes were determined in the following manner. The supercoiled plasmid pTZ19R was linearized with *Eco*RI. After complete digestion of the plasmid with *Eco*RI (confirmed by agarose gel), the DNA was subjected to ethanol precipitation and drying. The DNA prepared in the above manner was used for the different reagent-induced DNA cleavage experiments.

The DNA cleavage reaction conditions for the sequencing experiments were similar to those employed in the agarose gel assays (described above) except that a total reaction volume of 50 μL and 2 μg of plasmid/reaction were used. After incubation for 5 min, 10 μL of the reaction mixture was aliquoted and analyzed by gel electrophoresis on agarose to confirm the reagent-induced DNA cleavage. The residual reaction mixture was first subjected to ethanol precipitation and then dried under vacuum. The dry DNA pellets were then resuspended in water and used as templates for the primer extension reactions. The primer extension reactions were carried out by the adaptation of a literature procedure (*28*). Briefly, ~3 pmol of the ^{32}P-end-labeled primer (300 000 counts, a 19-mer oligonucleotide) and 4 μL of 0.01 M NaOH were added into a solution containing ~0.5 μg of the DNA templates. Then, the volume of the resulting reaction mixture was made up to 40 μL which after thorough mixing was kept at 80 °C for 2 min and finally left on ice for an additional 5 min. Into this ice-cold reaction mixture was added 5 μL of the primer extension buffer [0.5 mM Tris-HCl (pH 7.4), 0.1 M $MgSO_4$, and 2 mM DTT], and the resulting mixture was again incubated at 45 °C for 3 min. After this, the mixture was kept on ice for a period of 30 min. Then, an aliquot of 5 μL of the dNTP mix (dATP, dTTP, dCTP, and dGTP each at 5 mM) was added to this mixture, and primer extension reactions for each reaction were initiated by the addition of 1 unit of Klenow DNA polymerase at 50 °c for 10 min. Finally, the reactions were quenched by the successive addition of 10 μL of 4 mM ammonium acetate/20 mM EDTA and 180 μL of absolute EtOH. The resulting mixture was then kept at −20 °C for 1 h and pelleted down by centrifugation. The pellets thus obtained were air-dried and resuspended in 8 μL of 80% formamide-denaturing gel loading dye, heated for 2 min at 92 °C, then loaded onto a 7% polyacrylamide−bisacrylamide/8 M urea denaturing sequencing gel, and finally electrophoresed at 1500 V until the bromophenol blue touched the foot of the gel (~2 h). Then, the gel was autoradiogrammed.

RESULTS AND DISCUSSION

Choice of the Ligand. The tetradentate chelator salen [*N,N′*-ethylene bis(salicylideneaminato)] has been widely employed for various purposes in the chemical literature (*29*) over a long period of time. The utilities of several metal−salen complexes in effecting catalytic, regioselective alkene epoxidation have also been demonstrated (*30*). Recently, Griffin *et al*. examined in detail the DNA scission activities of an array of Mn(III)−salen derivatives (*16*). Preferential cleavages of DNA at A·T rich sites by the Mn(III)−salen reagents such as **5** were observed in the presence of the co-oxidant, magnesium monoperoxyphthalate (MMPP). Due to our continuing interest in the studies of metal complex systems that bind DNA and induce DNA scission (*19*), we sought to examine systematically the interactions that exist between individual transition metal−salen with DNA under comparable conditions. Since salen itself is not soluble in water, we first chose to functionalize the parent salen unit by covalent appendages with two NMe_3^+ residues (ligand, **1**). This renders the ligand (**1**) and its different metal complexes water-soluble irrespective of the pH of the solution. This also allows these compounds to come closer to the DNA surface due to the favorable electrostatic disposition. It should be mentioned, however, that the idea of the introduction of the cationic residues into salen is not new. Burrows and Rokita (*17*) developed a bis-cationic Ni(II)−salen derivative which was shown to induce interstrand cross-linking in DNA. Subsequently, Sato *et al*. used a different cationic salen type Cu(II) complex to examine their DNA binding abilities (*15*). More recently, Bailly and Bernier examined the interactions and the DNA-cleaving properties of the salen−Cu(II) complex containing a pendant alkyl ammonium residue (*18*). To find the effects of the role of other ligand charges around the metal complexes, two anionic ligands and their corresponding metal complexes (**3** and **4**) have been also synthesized. The syntheses of the ligands and different metal complexes are summarized in Scheme 1.

Synthesis. The synthesis of the ligand **1** began with the functionalization of 4-hydroxybenzaldehyde with 1,3-dibromopropane in the presence of $KHCO_3$ in dry acetone under refluxing conditions. The product, 4-[(3-bromopropyl)oxy]salicylaldehyde (**6**), thus obtained was quaternized quantitatively upon reaction with Me_3N in EtOAc. The counterion of the quaternary salt was changed to perchlorate by treatment with $NaClO_4$, and then the perchlorate salt was converted to the corresponding salen (**1**) in 80% yield upon coupling with ethylenediamine in MeOH. Different metal complexes of this ligand were synthesized on treatment with appropriate metal salts in MeOH. The ligand **3** was prepared by coupling 3,4-diaminobenzoic acid with salicylaldehyde in MeOH, and the corresponding Ni(II) complex was synthesized upon treatment with $NiCl_2$ in MeOH. For the preparation of salens with pendant negatively charged residues, 4-hydroxysalicylaldehyde was coupled with ethyl 6-bromohexanoate in acetone in the presence of $KHCO_3$. This gave **7** in ~50% yield upon chromatographic purification. **7** was then saponified to the corresponding acid (80%) which upon conversion into imine with ethylenediamine gave the bis-anionic salen **7b** in 90% yield. This on complexation with $NiCl_2$ in a mixture of MeOH/$CHCl_3$ afforded the salen **4** in *ca*. 70% yield. All the final compounds and the intermediates were characterized by UV−vis, FTIR, and ^{1}H-NMR spectroscopy and by elemental analysis. The details of the synthesis and characterization of each of the new compounds are given in Experimental Procedures.

Absorption Titration. DNA appears to be a convenient target for different metal complex-based reagents (*31*) as most of the metal complexes contain a variety of potential DNA binding loci. The presence of the nucleobases with ligating abilities and phosphodiester linkages offers scope for direct coordination with a central metal ion in a complex. Furthermore, the coordinatively "unsaturated" sites on the metal ion centers of these complexes may also promote cross-linking at different regions within a long DNA strand or between different strands. In addition to these, other modes of interaction such as ion pairing or hydrogen bonding to minor or major grooves of the DNA and the intercalation of the planar aromatic subunits of some of these complexes into the stacked base pairs may also be possible. The above considerations make it clear that in principle it should be possible to modulate the binding and reactivities of the transition metal complexes with DNA by changing

Scheme 1

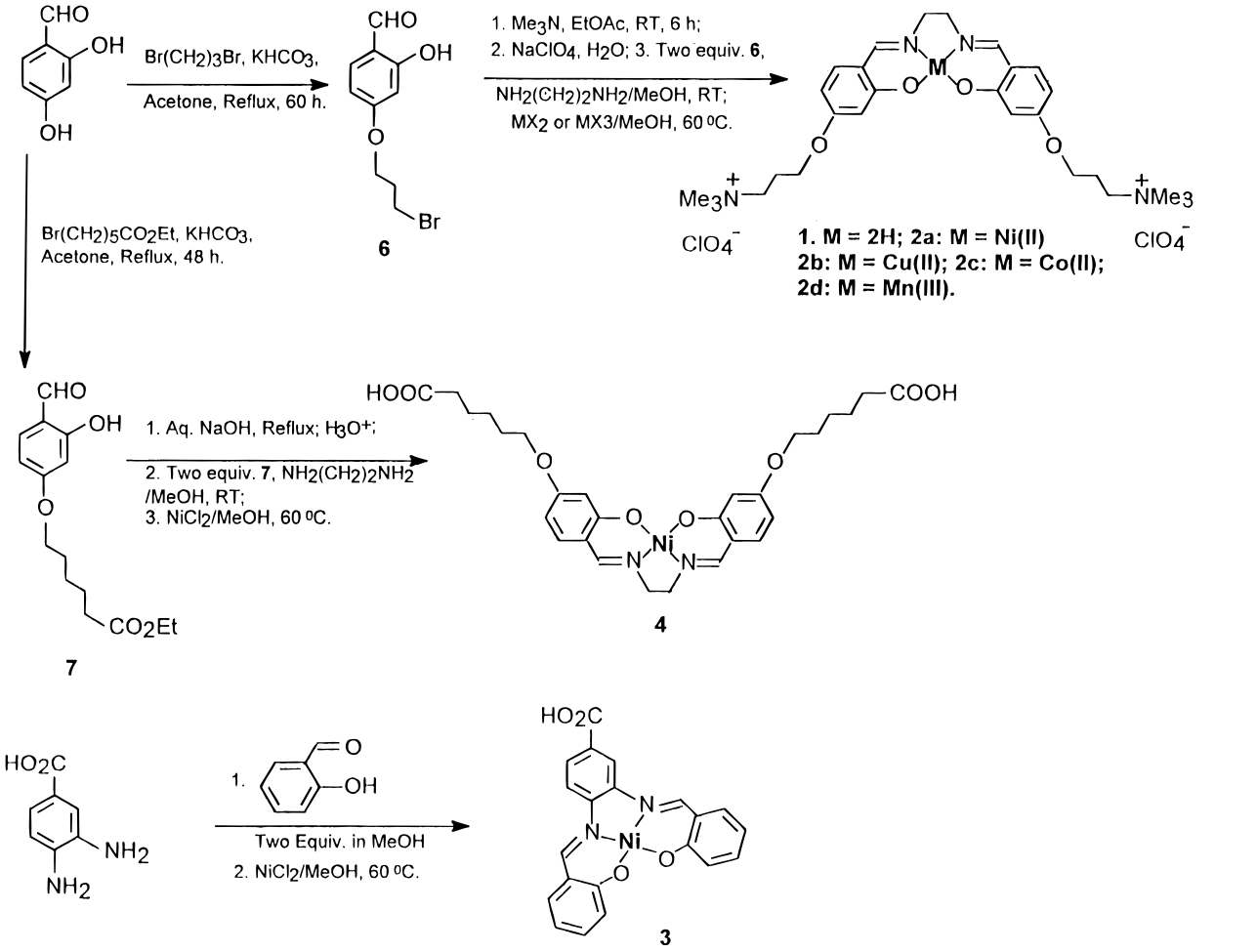

the central metal ion, its oxidation state, and the electrostatic character of the ligands of the metal complexes.

In the present study, we investigated the interactions between the newly synthesized salen complexes with DNA. The binding of salen derivatives (**1**) and its various metal complexes to duplex DNA led to decreases in the absorption intensities with a small amount of red shifts in the UV−vis absorption spectra of the salen species. Figure 1 shows the absorption spectra of the bis-cationic salen analogue **1** and its various metal complexes in the presence and absence of varying concentrations of *E. coli* genomic DNA. Absorption titrations with a given compound were carried out by adding increasing amounts of *E. coli* genomic DNA of a known concentration into a solution [Tris-HCl buffer (pH 7.4)] containing a fixed concentration of the metal complex or the ligand by following changes in the UV−vis spectroscopy after each addition. The addition of DNA was continued until a saturation in the observed spectral changes for a given system was reached. The absorption titration of different metal complexes or the ligand with *E. coli* genomic DNA allowed us to obtain estimates of the binding constants of the individual metal complexes with DNA.

Curve 1 in Figure 1A shows the UV−vis spectrum due to an aqueous solution (pH 7.4 Tris buffer) containing 2.14×10^{-6} M ligand **1** alone in the absence of DNA. Curves 2 and 3 show spectra due to **1** manifested upon addition of increasing amounts of *E. coli* genomic DNA. It is clear that the progressive addition of DNA leads to strong hypochromism in the absorption intensity of **1** finally reaching a saturation at $P/D = 2.3$, where P is the concentration of the DNA in phosphate molarity and D is the concentration of the compound used in the study (ligand, **1**). The saturation plot obtained by plotting A_0/A against [DNA] due to this titration is also given (inset of Figure 1A).

Panels B−D of Figure 1 show the results of the UV−visible absorption titration of bis-cationic metal complexes **2a**−**c**, respectively, in the presence of increasing amounts of *E. coli* genomic DNA. Spectral trace 1 in all of these panels represents the UV−vis absorption spectra of metal complexes **2a**−**c**, respectively, in pH 7.4 Tris buffer in the absence of any DNA. In each instance, the addition of progressively increasing amounts of DNA resulted in gradual hypochromism in the absorption intensities of the respective metal complexes which finally reached saturation. The insets in panels B−D of Figure 1 show the corresponding saturation plots.

The results of the absorption titration in the presence of progressively increasing amounts of DNA with either tricationic Mn complex **2d** or monocationic Mn complex **5** are shown in panels E and F of Figure 1, respectively. In either of these cases, spectrum 1 (in the absence of DNA) gradually changed to traces 2 and then to 3 upon addition of increasing amounts of DNA. Continuous decreases in the intensities of absorption due to **2d** or **5** were followed by saturation at high concentrations of DNA (insets in panels E and F of Figure 1, respectively).

Isosbestic points are clearly observed in panels A (~290 and ~305 nm), B (~330 nm), C (~290 nm), D (~300 nm), and F (~260 and ~330 nm) of Figure 1 for binding of respective salens with DNA. The presence of the isosbestic points in these titrations suggests that chemical

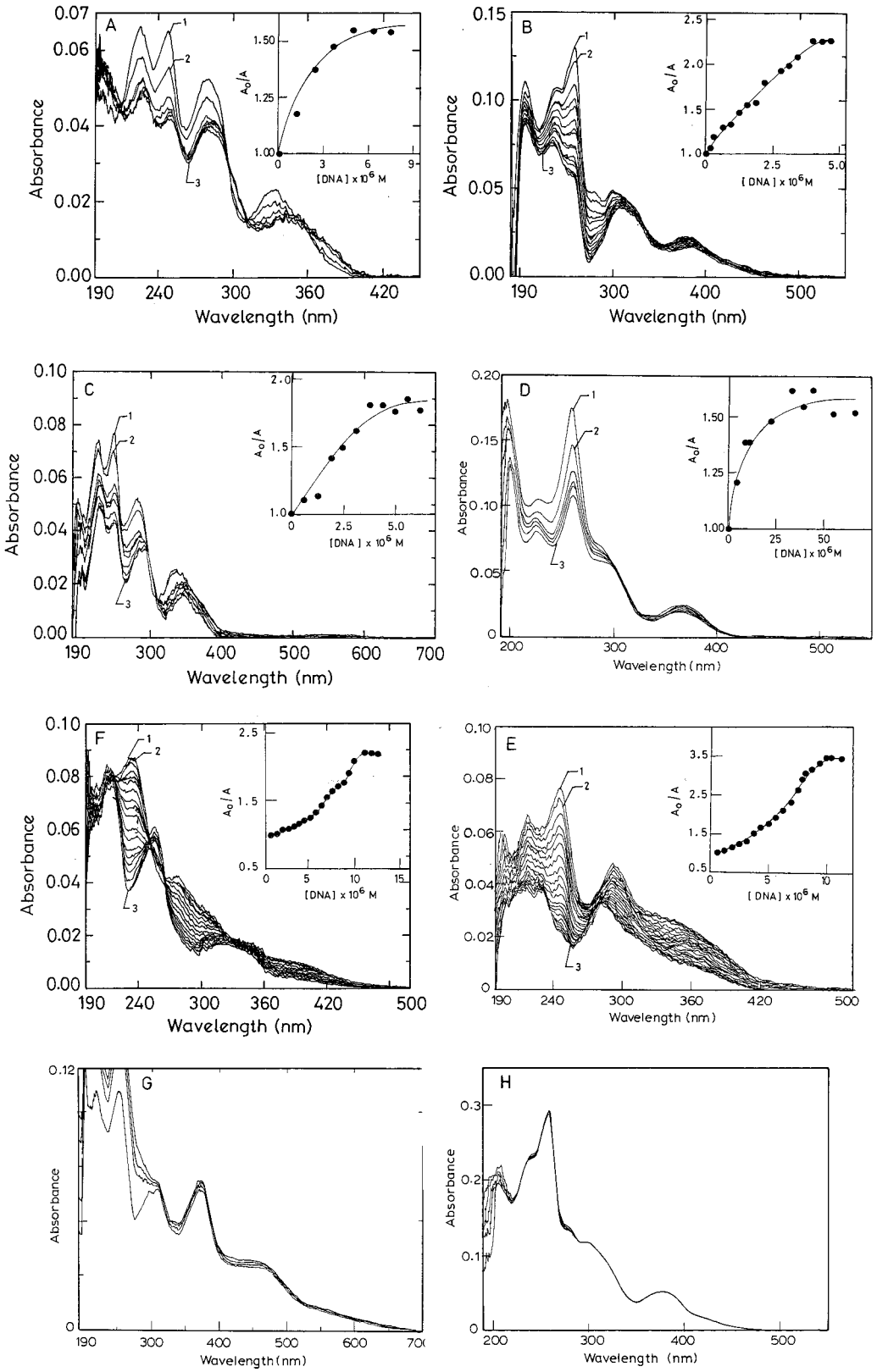

Figure 1. Absorption titration spectra of the ligand and different metal complexes in the presence of *E. coli* DNA. The absorption titrations were carried out by keeping the concentration of the complex constant while adding increasing amounts of *E. coli* genomic DNA until the saturation was reached. In all cases, spectrum 1 represents probe alone in the absence of any DNA; spectra 2 and 3 were obtained upon addition of increasing concentrations of DNA while keeping the probe concentration fixed. (A) **1** *vs* DNA. [**1**] = 2.14×10^{-6} M. (B) **2a** *vs* DNA. [**2a**] = 5.67×10^{-6} M. (C) **2b** *vs* DNA. [2b] = 2.6×10^{-6} M. (D) **2c** *vs* DNA. [**2c**] = 3.9×10^{-6} M. (E) **2d** *vs* DNA. [**2d**] = 2.56×10^{-6} M. (F) **5** *vs* DNA. [**5**] = 2.1×10^{-6} M. (G) **3** *vs* DNA. [**3**] = 5.7×10^{-6} M. (H) **4** *vs* DNA. [**4**] = 7.19×10^{-6} M. (Insets) Respective saturation plots. The saturation in absorption intensity hypochromism is indicated by the plot of A_o/A *vs* [DNA] in phosphate molarity, where A_o and A are the absorption intensities in the absence and in the presence of varying concentrations of DNA, respectively.

equilibria exist between the bound and the free metal complexes or the ligand with no spectroscopically detectable intermediate states in the presence of DNA in each of the above instances. Strong hypochromism and spec-

Table 1. UV−Vis Absorption Spectral Properties of Metallosalens and Metal Free Ligand in the Presence and Absence of *E. coli* Genomic DNA[a]

compound	wavelength maxima (nm)[b] free	wavelength maxima (nm)[b] bound	% hypochromism[c] (λ_{max}, nm)
1	335, 281, *248*	344, 282, 251	30 (335), 20 (281), 33 (248)
2a	381, *259*	389, 260	18 (381), 57 (259)
2b	336, 282, *249*	345, 292, 250	54 (336), 31 (282), 43 (249)
2c	262, *258*	262, 253	25 (262), 34 (258)
2d	293, 245	293, 248	45 (293), 71 (245)
3	450, 372, 300, 250	*d*	*d*
4	376, 258	*d*	*d*
5	280, 237	280, 237	55 (237)

[a] See the text for the details of the experimental conditions. [b] Upon binding with DNA, the λ_{max} due to the bound complex which was used for the construction of half-reciprocal plots is italicized. [c] *E. coli* genomic DNA was purified by the phenol−chloroform extraction as described in the text. [d] No significant spectral changes were observed.

tral broadening in absorption intensity indicate intense interaction between the electronic states of the complex chromophore with that of DNA bases.

Panels G and H of Figure 1 show the UV−visible absorption titration spectra for the *monoanionic* and the dianionic Ni complexes **3** and **4**, respectively, with DNA. Interestingly, in either of these instances, small or no significant spectral changes were observed upon addition of increasing amounts of DNA to solutions containing the above anionic metal complex **3** or **4**.

Experimentally determined parameters from the absorption titration for the different free and DNA-bound metal complexes as well as the metal free ligand are collected in Table 1. The data clearly demonstrate that the electronic spectra of all the cationic metal complexes as well as those of the bis-cationic, water-soluble, metal free ligand are indeed significantly affected upon binding to DNA. This is in marked contrast with the absorption titration involving the anionic metal complexes in the presence of increasing amounts of DNA (panels G and H of Figure 1).

The structural characteristics of compounds **1** and **2a**−**d** are such that each of them is dicationic in the bivalent oxidation state of the central metal ion. Ligands in such complexes have positively charged residues through a short spacer chain [$(CH_2)_3NMe_3^+$]. These pendant NMe_3^+ residues remain positively charged irrespective of the pH and anionic strength of the media. Thus, the overall positively charged character of the metal complexes provides the basis for electrostatic binding of these compounds with polyanionic DNA.

Under our experimental conditions, the bis-cationic metal complexes, including that of Cu(II), showed strong interaction with DNA as shown by the pronounced hypochromism and red shift. This is in contrast to the observation reported in the DNA binding studies of the Cu(II)−salen analogue by Sato *et al*. It is noteworthy that the ionic strength (50 mM) used by Sato *et al*. was much higher than the one used in the present study. Binding of several other metal chelates with DNA was previously shown to depend on the ionic strength of the media in which the titration experiments were conducted.

Binding Constants of Salen−DNA Association. The association constants of different metal complexes or the ligand with DNA were calculated by employing the method (half-reciprocal plot) using eq 1 as described previously (*cf*. Experimental Procedures). The half-reciprocal plots for different compounds were constructed using the most affected wavelength maxima as determined from the respective absorption titration experiments. Importantly, the plots of $D/\Delta\epsilon_{ap}$ *vs* D resulted in straight lines (Figure 2) for the absorption titration of **1** and **2a**−**c** with DNA. Individual association constants due to DNA binding with **1** and **2a**−**c** are given in Table 2. It is important to note that under comparable conditions, however, when the absorption titration data of either **2d** or **5** in the presence of DNA were plotted, the resulting fits did not give linear (straight) half-reciprocal plots. Thus, the saturation plots corresponding to Mn complexes **2d** and **5** (insets of panels E and F of Figure 1, respectively) differed from the other saturation plots given in the insets of panels A−D of Figure 1 with other metal complexes or the ligand **1**. These findings suggest that the binding mode of either of these manganese-based metal complexes (**2d** and **5**) with DNA relative to that of the free ligand or its Co(II), Cu(II), or Ni(II) complex counterparts could be different, although all of the salen complexes showed strong absorption hypochromicities as long as the compounds contained net cationic charge. Similar differences were also apparent while the effects of inclusion of these metal complexes on the DNA melting were examined (see below).

Effect of the Addition of Salt on DNA Binding. To elucidate the influence of the ionic strength on the DNA binding abilities of the above metal complexes, we then studied the effects of the addition of increasing amounts NaCl and $MgCl_2$ on the DNA binding of one of the above metal complexes, *e.g*. **2b**. This experiment was performed by progressive addition of several aliquots of concentrated solutions of either NaCl or $MgCl_2$ into a solution containing fully DNA-bound **2b**. In Figure 3, spectral trace 1 respresents the UV−vis absorption spectrum due to the solution containing **2b** alone (2.63 μM), in the absence of DNA. Spectrum 2 in Figure 3 shows the UV−vis absorption spectra of fully DNA-bound **2b** obtained upon addition of excess CT DNA to the solution containing **2b**. Traces 3 and 4 were obtained upon addition of 30 and 45 mM NaCl to the **2b**−DNA complex. Thus, addition of increasing amounts of NaCl into the **2b**−DNA complex led to an apparent hyperchromism in the absorption intensities of **2b** finally reaching a saturation. While further addition of NaCl did not lead to any spectral changes, addition of a concentrated aqueous solution of $MgCl_2$ into the above led to further hyperchromism (trace 5, [$MgCl_2$] = 15 mM).

In a separate experiment, we also examined the effect of the addition of several aliquots of aqueous solutions of $MgCl_2$ to a solution containing the **2b**−DNA complex (figure not shown). Upon addition of increasing amounts of $MgCl_2$, the apparent hyperchromism in the absorption intensities of the metal complex was observed, finally reaching a saturation. To obtain the same extent of hyperchromism in absorption intensities of the DNA-bound **2b**, nearly half the concentration of $MgCl_2$ was required compared to that of NaCl. Notably, the saturation in the hyperchromism in the absorption intensities of the DNA-bound **2b** obtained by the addition of excess $MgCl_2$ could not be altered by further addition of NaCl.

The hyperchromism observed upon addition of increasing amounts of salt to salen-bound DNA could be explained by considering the enhanced charge neutralization of the negatively charged DNA in the presence of the metal ion of the salt (*26*). This charge neutralization minimizes the intra and interstrand repulsion between the DNA double helix, promoting the formation of more "compact" DNA structure. Under these circumstances, the average distance between base pairs is decreased. This makes the accommodation of **2b** into the duplex DNA difficult. The dicationic nature of Mg^{2+} ion

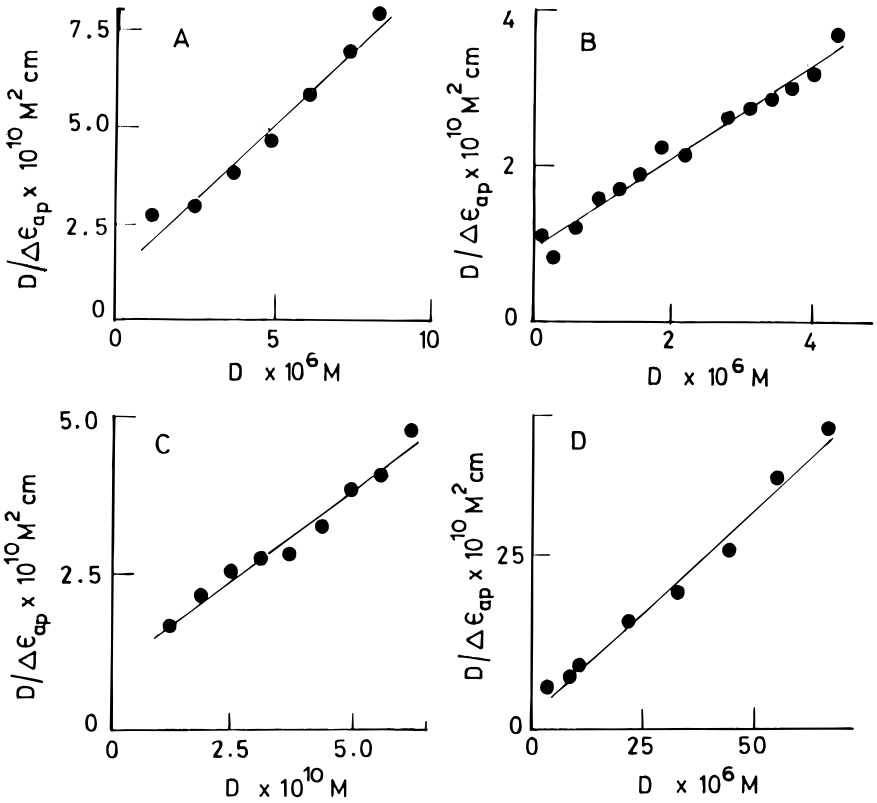

Figure 2. Half-reciprocal plots for binding of different complexes with *E. coli* DNA. The half-reciprocal plots for different complexes were obtained by plotting $D/\Delta\epsilon_{ap}$ *vs D* according to eq 1 as described in Experimental Procedures. Panels A–D show the half-reciprocal plots for DNA binding due to **1** and **2a**–**c**, respectively. The binding constants for **1** and **2a**–**c** were calculated as 3.6×10^5, 5.2×10^5, 6.0×10^5, and $10.0 \times 10^5\ M^{-1}$, respectively, by taking the corresponding ratio of the slope to *y*-intercept.

Table 2. Binding Constants and Related Parameters for DNA–Metallosalen Association[a]

compound	10^6[compound] (M)[b]	10^6[DNA][c] (M)	$10^{-5}K$[d] (M^{-1})
1	2.1	8.4	3.6
2a	5.7	4.3	5.2
2b	2.6	6.2	6.0
2c	3.9	70.0	10.0
2d	2.6	11.1	*e*
3	5.7	50	*f*
4	7.2	180	*f*
5	2.2	12.4	*e*

[a] For binding constant determination, see the text for details. [b] The concentrations of the compounds were fixed at the given values. [c] Saturating concentration of DNA. [d] *K* was determined from the ratio of the slope to the *y*-intercept of each of the half-reciprocal plots as described in Experimental Procedures. We estimate that the values determined for *K* for the titration experiments are within ±5%. [e] Interpolation of the binding titration data did not result in a linear half-reciprocal plot, and hence, binding constants could not be calculated. [f] No significant binding was observed.

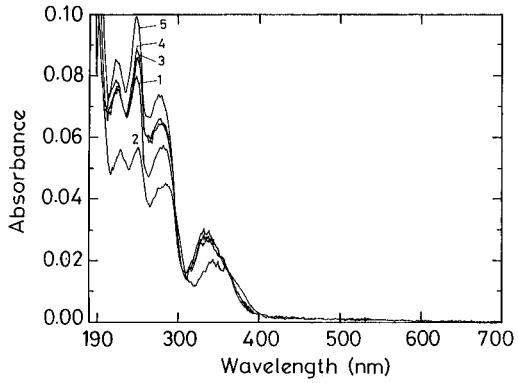

Figure 3. Effect of the addition of salt on DNA binding. This was performed by examining the UV–vis spectra upon addition of progressively increasing amounts of various salts to a **2b**–DNA complex solution: trace 1, **2b** alone, [**2b**] = 2.63×10^{-6} M; and trace 2, with excess CT DNA, [DNA] = 5.83×10^{-6} M in base molarity. Traces 3 and 4 contain the **2b**–DNA complex in the presence of 30 and 45 mM NaCl. Trace 5 contains the **2b**–DNA complex in the presence of 15 mM $MgCl_2$.

affects the charge neutralization of DNA twice as effectively as the monocationic Na^+ ion. This explains why at nearly 50% concentration of $MgCl_2$ relative to that of NaCl the same extent of hyperchromism in absorption intensities of the **2b**–DNA complex could be attained. Taken together, all of the above observations suggest that intercalation may be important, but all of the above can also be explained on the basis of charge neutralization and may also involve groove binding or phosphate binding.

Binding of the Salen 2a to Denatured DNA. In the present study, we compared the binding ability of the Ni complex **2a** toward the double-stranded DNA as opposed to that with alkali-denatured DNA. The double-stranded CT DNA was denatured using concentrated, aqueous NaOH. Trace 1 (Figure 4) stands for the complex **2a** (3.35 μM) alone in the absence of DNA. Spectral trace 2 is obtained after the addition 5.83 μM (base molarity) alkali-denatured CT DNA (pH ~11) to **2a**. Under these conditions, the absorbance peak at 259 nm was reduced by about ~65% compared to that observed with native double-stranded CT DNA. The decrease in the pH of this solution by progressive addition of small aliquots of aqueous HCl solution led to successive increases in hypochromism reaching a minima (~55%) at around pH 7 (traces 3–8).

The initial, small extent of hypochromism observed in the absorption intensity of the Ni complex **2a** in strongly alkaline media even in the presence of excess DNA suggested a weak binding of the probe **2a** with the

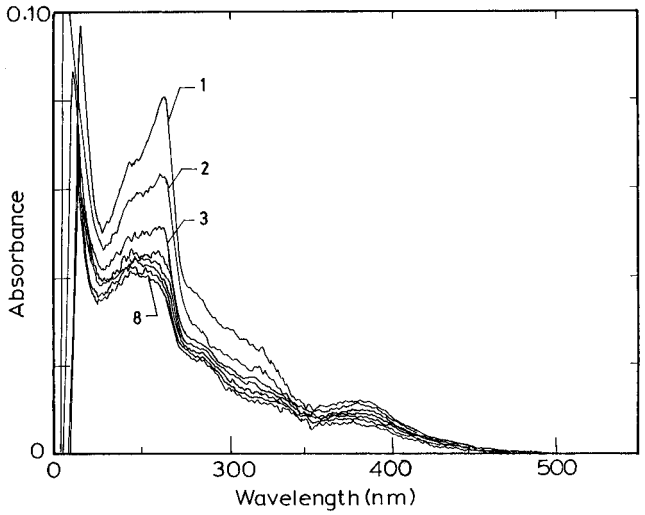

Figure 4. Binding of **2a** to denatured DNA. This was performed by adding an aliquot of alkali-denatured CT DNA into solution of **2a**. An absorption spectrum was recorded, and the same was followed by addition of increasing amounts of aqueous HCl to this mixture to allow progressive slow renaturation. Trace 1 is for **2a** alone in the absence of any DNA; [**2a**] $= 3.35 \times 10^{-6}$ M. Trace 2 shows UV−vis the spectrum of **2a** in the presence of 5.83×10^{-6} M CT DNA ([NaOH] $= 5.0 \times 10^{-3}$ M). Traces 3−7 were obtained by adding successively each time 1.5 μL of 0.6 M aqueous HCl.

denatured CT DNA. Increasing amounts of HCl addition decrease the pH of the solution by making the conditions more favorable for the renaturation of DNA. Under these circumstances, the formation of more double-stranded DNA duplexes was therefore facilitated. The increase in hypochromism with decreasing pH therefore indicates that there is stronger electronic interaction of the Ni complex with double-stranded DNA upon renaturation. This is in complete agreement with the fact that the absorption hypochromism was maximal at pH ~7 where the DNA is present predominantly in the renatured form. A further decrease in pH (below 6.5) also results in the protonation of the DNA bases. Under these circumstances, there is a strong distortion in the DNA structure (*32*). This was reflected in the reduction in hypochromism with a further decrease in pH (not shown). Taken together, these results clearly demonstrate that the salen **2a** does not physically bind to single-stranded DNA to the extent it does with native duplex DNA.

Effects of Salen Binding on DNA Melting. Additional information concerning the role of DNA binding by different metallosalens was available from the thermal denaturation studies. The melting temperature studies clearly demonstrate that strong interactions between the different cationic metal complexes with CT DNA. The melting profiles of CT DNA in the absence and presence of various metal complexes are shown in Figure 5. Curve 1 in Figure 5 shows the melting profile of 72 μM CT DNA alone (T_m ~ 62 °C) in 5 mM Tris-HCl buffer (pH 7.4). Curves 2−6 show the melting profiles of the CT DNA in the presence of **2a** (1.7×10^{-5} M), **2b** (1.6×10^{-5} M), **2c** (2.1×10^{-5} M), **2d** (2.6×10^{-5} M), and **5** (2.6×10^{-5} M), respectively. These experimentally determined melting temperature data for CT DNA in the absence and presence of different metal complexes are given in Table 3. The binding of either of **2a** or **2b** to DNA led to the enhancement of the melting temperature by ~18 and ~10 °C, respectively, from that of the DNA alone, and the corresponding melting profiles were also found to be sharp. So the binding of either **2a** or **2b** increased the thermal stability of DNA duplexes as shown by the enhancement in the T_m values of CT DNA in the presence

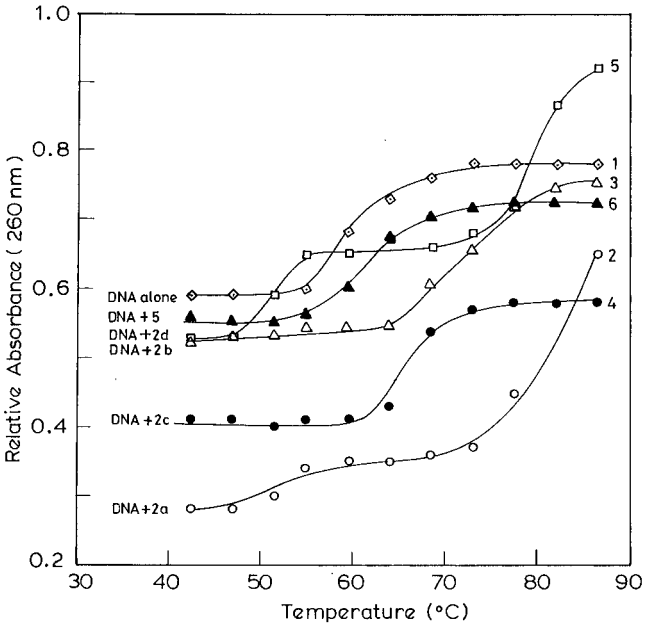

Figure 5. Effect of the inclusion of different metal complexes on the melting of CT DNA. Melting profiles of CT DNA in the presence or absence of different compounds were obtained by plotting the changes in the absorption intensities at 260 nm as a function of temperature. These experiments were carried out with 72 μM (bM) CT DNA with 5 mM Tris-HCl at pH 7.4: curve 1, CT DNA alone; and curves 2−6, melting profiles of CT DNA in the presence of **2a** (1.74×10^{-5} M), **2b** (1.63×10^{-5} M), **2c** (2.09×10^{-5} M), **2d** (2.59×10^{-5} M), and **5** (2.63×10^{-5} M), respectively.

Table 3. Melting Transitions for Calf Thymus DNA in the Presence of Various Metallosalen Complexes[a]

entry	probe	10^5[probe][b]	T_m (°C)[c]
1	*d*	*d*	62
2	**2a**	1.74	80
3	**2b**	1.63	72.5
4	**2c**	2.09	67.5
5	**2d**	2.59	79, 51
6	**5**	2.63	62

[a] The DNA melting was carried out at a DNA concentration of 72 μM (base molarity). [b] The concentration of the salen used. [c] The melting temperatures were obtained in the presence of salen and are within ±1 °C. [d] Melting temperature of the DNA alone.

of these compounds. This enhancement in melting temperatures could be due to intercalative binding of the metal complexes with DNA, although other modes of binding are also possible. In the presence of **2d**, a complicated, apparently biphasic melting transition profile with one at ~51 °C and another one at ~79 °C was observed. This might indicate the differences in the mode with which **2d** interacts with DNA as opposed to **2a**−**c**. The melting profile of DNA in the presence of **5** becomes slightly broadened, although the melting temperature did not change significantly.

In **2a** and **2b**, the pendant positive charges (away from the metal complex core) bring them closer to DNA on electrostatic grounds, leaving the neutral, flat, aromatic region of the complex favorably disposed for further interaction with DNA duplexes. These features in **2a** and **2b** probably contribute to the significant enhancement in DNA melting temperatures. But in the case of Mn(III) complexes **2d**, the complex core bears additional positive charge which probably alters the mode of binding of such complexes with DNA. That is why we see either insignificant changes in T_m upon binding of **5** with DNA or a more complex biphasic DNA melting profile with tricationic **2d**. In the case of Co(II) complex **2c**, the

increase of the DNA melting temperatures was found to be ~5 °C. It is important to note that, in order to bring a comparable magnitude of absorption hypochromicity, a DNA concentration nearly 1 order of magnitude greater was necessary with this complex relative to that of **2a** and **2b**. The exact reasons for the somewhat modest increases in the DNA melting temperature and the requirement of a higher concentration of DNA during absorption titration are difficult to interpret adequately at this time. However, it could be (i) due to the ability of **2c** to promote DNA scission even in the absence of co-oxidants and (ii) owing to its high oxygen binding capacity (*24*) the resulting complex may also adopt a nonplanar shape. This deviation from planarity could alter the mode of its interaction with DNA.

DNA Cleavage Studies. The DNA cleavage abilities of different metal complexes in the presence and absence of co-oxidants were investigated with the aid of electrophoresis on agarose gel by noting the conversion of the supercoiled plasmid (form, **I**, *FI*) to a nicked circle (form, II, *FII*) and then to the completely linear form (form III, *FIII*). As shown in Figure 6A, compounds **2a**, **2d**, and **5** were able to induce oxidative cleavages of DNA. Incubation of the plasmid DNA pTZ19R at 37 °C for 5 min with 10 μM **2a**, **2d**, and **5** in the presence of MMPP caused appreciable conversion of form I to the nicked circular form II (lanes 9, 7, and 5, respectively, in Figure 6A). The use of higher concentrations of these reagents (0.1 mM) and longer incubation (>15 min) with DNA resulted in double-strand cleavages or even complete degradation (smears) of DNA (figure not shown). Densitometric examination revealed that the DNA nicking efficiencies of tricationic **2d** were a little higher than that of monocationic **5** under comparable conditions. Control experiments verified that any of the above metal complex by itself (in the absence of MMPP) could not affect detectable DNA scission. Significantly, compound **2b** did not show any DNA cleavage activity in the presence or absence of MMPP or any other oxidants, *e.g.* oxone or H_2O_2 (figure not shown). Even with low **2a** concentrations in the presence of MMPP, double-strand scission was appreciable. With the Co(II) complex **2c**, the situation was more complex. It did not appear to show significant DNA nicking when examined on an agarose gel either in the absence or in the presence of MMPP (lanes 10 and 11, respectively). However, more careful examination under a high-resolution sequencing gel confirmed that **2c** also induced considerable DNA modification in the absence of MMPP (see below).

To explore the possibilities of whether a mixture of a given metal ion and the water-soluble ligand **1** could induce DNA cleavage activity, we then went on to examine the DNA cleavage reactions *in situ* by mixing equimolar quantities of **1** with any one of the metal salts, and the reaction products were separated by agarose gel electrophoresis. Figure 6B shows the agarose gel for the DNA cleavage reactions carried out with various mixtures prepared *in situ* by adding individual metal ion to a solution of the ligand **1** in the presence and the absence of co-oxidant MMPP. Lanes 1 and 2 in Figure 6B contain supercoiled plasmid DNA pTZ19R alone and in the presence of 0.5/mM MMPP, respectively. Lanes 3, 4, 8, 12, and 15 contain 50 μM **1**, manganese(II) acetate, nickel(II) chloride, cobalt(II) acetate, and copper(II) acetate, respectively, in the presence of 0.5 mM MMPP. Lanes 5, 9, and 16 contain 50 μM mixtures of Mn(II), Ni(II), and Cu(II), respectively, with 50 μM **1** in the absence of MMPP. Lanes 6 and 7 contain DNA treated with 10 and 50 μM *in situ*-prepared Mn(II) complex, respectively, in the presence of MMPP. Lanes 10 and 11 contain DNA in addition to 10 and 50 μM *in situ*-prepared Ni(II) complex in the presence of MMPP. Lanes 17 and 18 contained DNA treated with 50 μM of Cu(II) and Cr(III) complex (prepared *in situ*), respectively, in the presence of 0.5 mM MMPP. Lanes 13 and 14 contain 50 μM *in situ*-prepared Co(II) complex in the absence and presence of 0.5 mM MMPP, respectively. (C, bottom) DNA cleavages by Ni complexes of **2a**, **3**, and **4**. Lanes 1 and 2 contain the DNA alone and in the presence of 0.5 mM MMPP, respectively, Lanes 3, 5, and 7 contain DNA incubated with 10 μM **2a**, **3**, and **4**, respectively, in the absence of MMPP. Lanes 4, 6, and 8 contain DNA incubated with 10 μM **2a**, **3**, and **4**, respectively, in the presence of 0.5 mM MMPP.

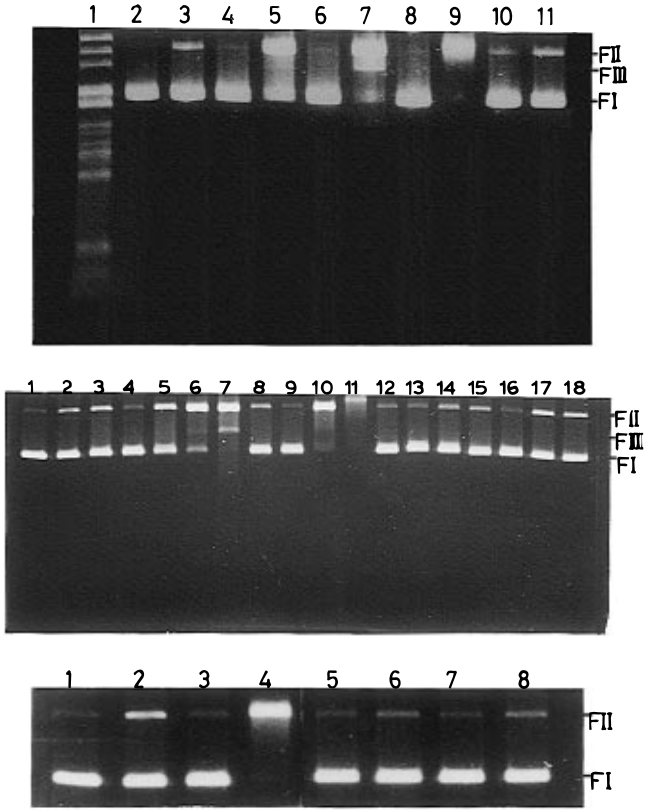

Figure 6. DNA cleavage studies and agarose gel assay. DNA cleavage abilities of the different metal complexes were examined using supercoiled plasmid pTZ19R (0.25 μg/reaction) in the presence and absence of 0.5 mM MMPP at 37 °C for 5 min in a 10 μL total reaction volume, and the reaction products were analyzed in 1% agarose gel and then stained with ethidium bromide and photographed. (A, top) DNA cleavages by different metal complexes. Lane 1 shows DNA molecular weight markers. Lanes 2 and 3 are supercoiled plasmid pTZ19R alone and in the presence of 0.5 mM MMPP, respectively. Lanes 4, 6, 8, and 10 contained the same DNA treated with 10 μM **5**, **2d**, **2a**, and **2c**, respectively, in the absence of MMPP. Lanes 5, 7, 9, and 11 contained the same DNA treated with 10 μM **5**, **2d**, **2a**, and **2c**, respectively, in the presence of 0.5 mM MMPP. (B, middle) DNA cleavages by different metal complexes prepared *in situ*. The different complexes were prepared *in situ* by mixing the water-soluble ligand, **1**, and the respective metal salts in equimolar quantities. Lanes 1 and 2 contain supercoiled plasmid DNA pTZ19R alone and in the presence of 0.5 mM MMPP, respectively. Lanes 3, 4, 8, 12, and 15 contain 50 μM **1**, manganese(II) acetate, nickel(II) chloride, cobalt(II) acetate, and copper(II) acetate, respectively, in the presence of 0.5 mM MMPP. Lanes 5, 9, and 16 contain 50 μM mixtures of Mn(II), Ni(II), and Cu(II), respectively, with 50 μM **1** in the absence of MMPP. Lanes 6 and 7 contain DNA treated with 10 and 50 μM *in situ*-prepared Mn(II) complex, respectively, in the presence of MMPP, and lanes 10 and 11 contain 10 and 50 μM *in situ*-prepared Ni(II) complex in the presence of MMPP. Lanes 17 and 18 contained DNA treated with 50 μM Cu(II) and Cr(III) complex (prepared *in situ*), respectively, in the presence of 0.5 mM MMPP. Lanes 13 and 14 contain 50 μM *in situ*-prepared Co(II) complex in the absence and presence of 0.5 mM MMPP, respectively. (C, bottom) DNA cleavages by Ni complexes of **2a**, **3**, and **4**. Lanes 1 and 2 contain the DNA alone and in the presence of 0.5 mM MMPP, respectively, Lanes 3, 5, and 7 contain DNA incubated with 10 μM **2a**, **3**, and **4**, respectively, in the absence of MMPP. Lanes 4, 6, and 8 contain DNA incubated with 10 μM **2a**, **3**, and **4**, respectively, in the presence of 0.5 mM MMPP.

metal free ligand nor the ligand free metal ions even in the presence of MMPP could induce any DNA nicking. The DNA nicking was observed only when Mn(II) and Ni(II) were treated with **1** in the presence of MMPP (lanes 6 and 7 and 10 and 11, respectively). In the presence of even micromolar concentrations of either Mn(II)−**1** or Ni(II)−**1** and MMPP, efficient DNA cleavages were observed. However, the combination of **1** with any of the Cu(II) (lane 17), Cr(III) (lane 18), Fe(II), or Zn(II) ions showed no detectable nicking even in the presence of MMPP.

It is evident that in this experiment it is possible to demonstrate that the DNA cleavage activities between the preisolated metal complexes and the metal complexes prepared *in situ* are quite similar. These results further demonstrate that it is indeed possible to modulate the reactivity of DNA cleavage by changing the central metal ion of a complex under the same ligand environment. Moreover, the DNA cleaving ability of different metal complexes could be monitored by using the metal complexes prepared *in situ* without requiring their prior preparation, purification, and characterization.

Role of the Charge on the Metal Complexes. In order to elucidate *the role of the charge* on the metal complexes toward the DNA cleavage reactions, the DNA modification abilities of monoanionic and dianionic Ni complexes **3** and **4** in the presence and absence of co-oxidant MMPP were examined. The results of these DNA cleavages were compared with that of the biscationic Ni complex **2a**. Figure 6C shows the comparative DNA cleavage abilities of **2a**, **3**, and **4**. Lanes 1 and 2 contained the DNA alone and in the presence of 0.5 mM MMPP, respectively. Lanes 3, 5, 7, contained DNA incubated with 10 μM **2a**, **3**, and **4**, respectively, in the absence of MMPP. Lanes 4, 6, 8 contained DNA incubated with 10 μM **2a**, **3**, and **4** respectively, in the presence of 0.5 mM MMPP. Thus, while in the presence of MMPP, the cationic Ni complex **2a** cleaves DNA efficiently (lane 4); neither monoanionic **3** nor the dianionic **4** induces and DNA scission under comparable conditions. This inability of **3** and **4** to induce DNA cleavage must be due to their unfavorable electrostatic character which impedes any significant interaction with the DNA. These results emphasize the fact that the presence of cationic charge around the reagent moiety is essential to bringing it close to DNA surfaces. Importantly, the inabilities of the anionic Ni complexes **3** and **4** to induce DNA modifications further suggest that the active species involved in the DNA cleavage processes described herein with the dicationic Ni complex are not diffusible in nature.

Primer Extension Assay and Autoradiogram. The examination of the DNA cleavage patterns produced by different metal complexes (shown below) has been confined only to those complexes that could apparently produce apparent single- and double-strand breaks in DNA on an agarose gel. The DNA modification patterns produced by the different reagents were examined by performing a primer extension assay. In this experiment, the primer is extended (by Klenow DNA polymerase) to the nick or any other modification in the DNA backbone. The products of this reaction were then analyzed on a high-resolution sequencing gel. Figure 7A shows the chemical modification patterns caused by 20 μM reagents (**2a**, **2d**, **2c**, and **5**) on the linearized plasmid pTZ19R. Although without appendages to DNA recognition matrices, we did not anticipate any profound selectivities in DNA modification, and we sought to find whether there was any selectivity in DNA modification by various reagents. Toward this goal, we performed the usual Sanger's sequencing parallel to primer extension reactions (lanes 1−4, G, A, T, and C, respectively.) Lanes 5 and 6 in Figure 7A are untreated DNA and with 0.5 mM co-oxidant MMPP, respectively. Lanes 7, 9, and 11 in Figure 7A contain 20 μM **5**, **2d**, and **2a**, respectively, without addition of MMPP. Lanes 8, 10, and 12 contain 20 μM **5**, **2d**, and **2a**, respectively, in the presence of 0.5 mM MMPP. Lanes 13 and 14 showed the DNA modification pattern produced by **2c**, in the absence of MMPP. Thus, these control experiments clearly showed that any of the metal complexes **2a**, **2d**, or **5** did not generate any cleaved products from the plasmid DNA without addition of any co-oxidants (Figure 7A, lanes 11, 9, and 7, respectively). We also found that reagents such as **2d**, **5**, and **2a** cleaved DNA efficiently even at 20 μM in the presence of 0.5 mM MMPP. The DNA cleavage efficiencies of **2d** and **5** were found to be comparable, while **2a** was found to be somewhat more efficient under comparable conditions. From the analysis of the autoradiogram in base levels, we found that both **2d** and **5** chemically modified in DNA with some selectivity (60−65%) toward the A·T regions of DNA duplexes and the selectivity for both the Mn(III) complexes are almost identical. These observations are consistent with the reports of Griffin in which it was already demonstrated that the related Mn(III)−salen complexes induce A·T selective DNA scission (*16*). In contrast, Ni(II) complex **2a** preferred to induce nicks in the G·C region (~70%) (*19a*). Thus, from these results it appears that it is also possible to change the selectivity of DNA modification to some extent by changing the central metal ion in a complex while keeping the ligand environment the same. These intrinsic selectivities, although modest, might indicate prior coordination to preferred base regions of the duplexes by the metal ions of **2a**, **5**, or **2d**. It is noteworthy that the Co complex **2c** alone also induced DNA modifications (without any co-oxidant MMPP) with little G selectivity (lanes 13 and 14, respectively). More significantly, in the presence of MMPP, **2c** did not cleave DNA at all (figure not shown). It is therefore apparent that **2c**-mediated DNA cleavage processes are not related to the DNA nicking events observed with Ni(II) or Mn complexes wich required the presence of co-oxidant MMPP.

The autoradiogram in Figure 7B shows the DNA cleavage pattern produced by **2d** and **2a**, respectively, toward supercoiled DNA and linearized DNA to elucidate the dependence of efficiencies and selectivities on secondary structures of nucleic acid. Lanes 6 and 8 in Figure 7B represent linearized and supercoiled plasmid pTZ19R alone, respectively. Lanes 2 and 4 show the supercoiled DNA after treatment with 5 μM **2d** and **2a**, respectively, in the absence of any MMPP. Lanes 1 and 3 contain supercoiled plasmid after treatment with 5 μM **2d** and **2a**, respectively, in the presence of 0.5 mM MMPP. Lanes 5 and 7 contain linearized DNA after treatment with 20 mM **2d** and **2a**, respectively, in the presence of 0.5 mM MMPP. Thus, it is quite clear that the efficiency of DNA cleavage produced by either of the reagents **2d** and **2a** was more on supercoiled DNA over its linearized counterpart at higher concentrations of the reagents are necessary for linearized DNA to produce a comparable cleavage pattern.

In order to independently confirm the results obtained from the primer extension reactions, we also carried out parallel control DNA cleavage experiments (not shown) ^{32}P-end-labeled double-stranded DNA fragments (approximately 200 bp). These results clearly showed that the Mn and Ni complexes could generate cleaved DNA fragments, although in the case of the Ni complex, few additional high-molecular weight bands possibly due to

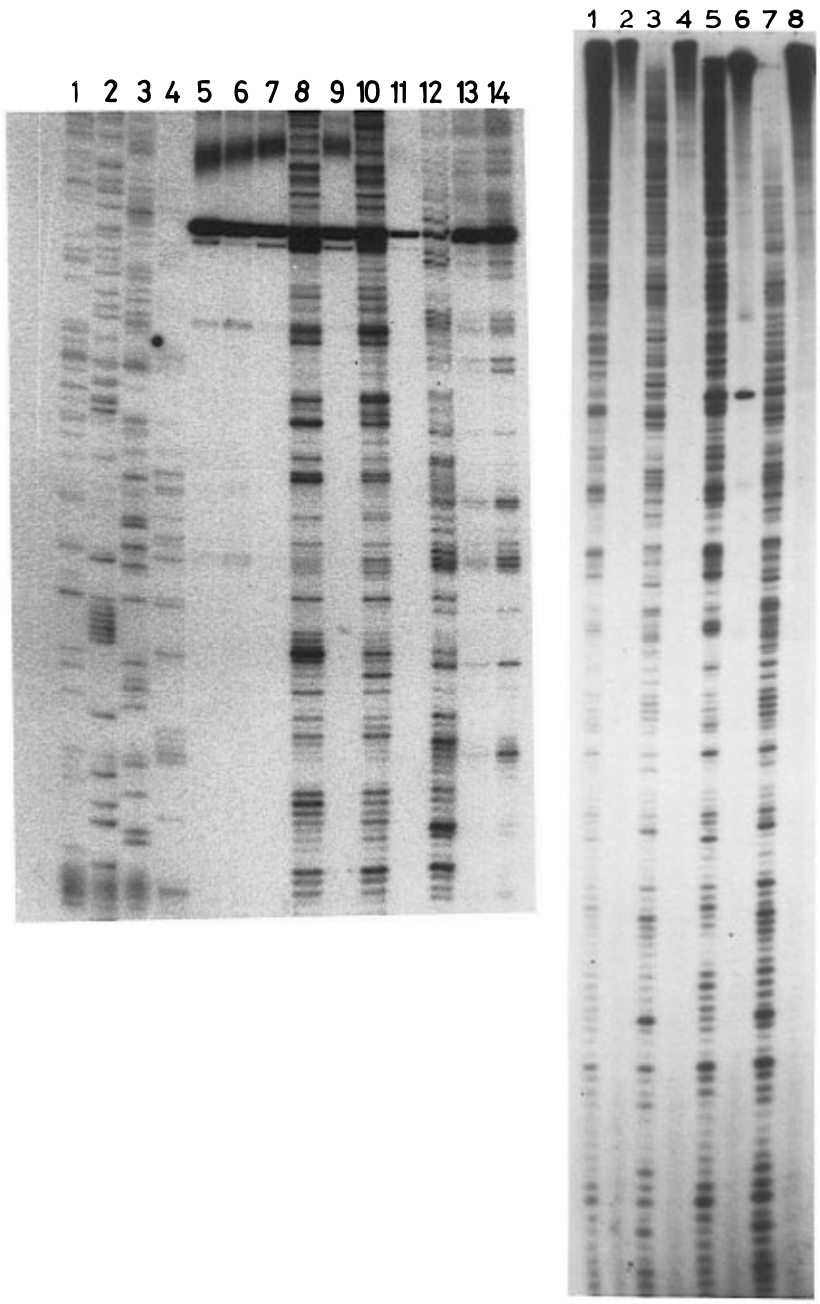

Figure 7. Sequencing and autoradiography. The sequence or the base specificities in DNA modification by different metal complexes in the presence and absence of different metal complexes were determined by performing primer extension. The ^{32}P-end-labeled primer was allowed on the chemically cleaved DNA fragments in the absence of any dideoxy nucleotide, and the primer extension products were analyzed on 8 M urea PAGE and autoradiogrammed. (A, left) DNA cleavage patterns produced by different metal complexes in the absence and presence of cooxidant MMPP. Lanes 1−4 are Sanger's sequencing reactions G, A, T, and C, respectively. Lanes 5 and 6 are untreated DNA and DNA with 0.5 mM MMPP, respectively. Lanes 7, 9, and 11 contain 20 μM **5**, **2d**, and **2a**, respectively, without addition of MMPP. Lanes 8, 10, and 12 contain 20 μM **5**, **2d**, and **2a**, respectively, in the presence of 0.5 mM MMPP. Lanes 13 and 14 show the DNA nicking pattern produced by 20 and 100 μM **2c**, respectively, in the absence of MMPP. (B, right) Structural (supercoiled *vs* linearized) dependence of DNA cleavage efficiencies for **2a** and **2d**. In lanes 6 and 8 are linearized and supercoiled plasmid pTZ19R alone, respectively. Lanes 2 and 4 are supercoiled DNA treated with 5 μM **2d** and **2a**, respectively, in the absence of any MMPP. Lanes 1 and 3 contained supercoiled plasmid treated with 5 μM **2d** and **2a**, respectively, in the presence of 0.5 mM MMPP. Lanes 5 and 7 contained linearized DNA treated with 20 μM **2d** and **2a**, respectively, in the presence of 0.5 mM MMPP.

reagent-induced cross-linking were also seen. The observation of the formation of cross-linked bands is consistent with earlier report of Burrows and Rokita (*17b, c*).

Possible Mechanism. The active species responsible for the DNA modification by the Ni complexes are probably derived from Ni(III) species. We assume therefore that the scheme proposed by Burrows (*17b*) persists in the present case also in which a related Ni−salen analogue was used. On this basis, we anticipate the involvement of an activated Ni(III) species for such profound DNA scission. We also examined the redox behavior of the Ni(II) complex under cyclic voltammetry (not shown). The complexes were found to undergo oxidative polymerization at the electrode surfaces. This finding also suggests a possible ligand−radical coupling involving the phenolic portion of the salen unit, where Ni(II) is oxidized to Ni(III) Goldsby *et al.* reached similar conclusions independently in their studies involving Ni(II)−bis(salicylaldimine) complexes (*33*). Formation of

ligand−radical should in part be responsible for the DNA cross-linking.

With regard to the chemistry of the Mn complexes, we feel that the DNA cleavages in these instances are affected in the following manner. The combination of the salen−Mn^{3+} and MMPP produces direct DNA nicks through pathways that do not require dioxygen. DNA cleavage releases free, unmodified nucleobases. Such observations are consistent with a plausible mechanism involving deoxyribose CH activation potentiated by an oxidatively activated species such as [salen−Mn(V)O]$^+$. The above suggestions are indeed supported in literature from the independent work of Griffin and others (*16b*, *34*).

The mechanistic pathways by which the Co(II)−salen−O_2-mediated DNA modification occurs is currently under investigation. Preliminary studies indicate that a superoxide radical-mediated active species is probably responsible for the observed DNA modification in this instance. In the presence of MMPP, the complex is oxidized to a Co(III) species which does not have ability to activate dioxygen, and hence, this does not possess DNA cleaving ability.

Concluding Remarks. In summary, we have developed several salen-based transition metal complexes which interact with or modify DNA. The binding and DNA modifications by such complexes can be modulated by the charge on the salen unit and more profoundly by the selection of the central metal ion. Only the salens with net cationic electrostatic character bind DNA, and the physical binding of the salen complexes does not occur to denatured (predominantly single-stranded) DNA to the extent that it does with native double-stranded DNA. Thus, probably a combination of the electrostatic and intercalative/groove binding interactions with DNA raise the duplex melting temperatures significantly. The anionic salens neither bind DNA nor induce strand scission irrespective of the central metal ion selected. The supercoiled forms of the plasmid DNA were found to be more susceptible to scission compared to their linearized forms by the cationic salens. Thus, to obtain comparable degrees of DNA cleavage, higher concentrations of the reagents were necessary with the linearized DNA.

The present findings demonstrate that modulation of the reactivities of the salen-based reagents toward DNA is possible and form a basis for further exciting studies. The newly introduced salen derivatives when tethered to suitable nucleic acid structural recognition matrices should be attractive as sequence specific reagents. Elucidations of the exact reaction conditions and mechanistic pathways for such important applications and also for the mapping of DNA tertiary structures are currently underway in our laboratory.

ACKNOWLEDGMENT

We are grateful to the referees for useful comments. S.S.M. thanks CSIR for a senior research fellowship. This work was supported by the funding from DST (INDO-HUNG to S.B.) and by the DBT and DST (to U.V.).

LITERATURE CITED

(1) (a) Sigman, D. S., Bruice, T. W., Mazumder, A., and Sutton, C. L. (1993) *Acc. Chem. Res. 26*, 98. (b) Barton, J. K., and Pyle, A. M. (1990) *Prog. Inorg. Chem. 38*, 413. (c) Burkhoff, A. M., and Tullius, T. D. (1988) *Nature 331*, 455. (d) Riordan, C. G., and Wei, P. J. (1992) *J. Am. Chem. Soc. 116*, 2189.

(2) (a) Tan, J. D., Hudson, S. E., Brown, S. J., Olmted, M. M., and Mascharak, P. K. (1992) *J. Am. Chem. Soc. 114*, 3841. (b) Nagai, K., Carter, B. J., Xu, J., and Hecht, S. M. (1991) *J. Am. Chem. Soc. 113*, 5099. (c) Nicolau, K. C., Maligres, P., Shin, J., de Leon, E., and Rideout, D. (1992) *J. Am. Chem. Soc. 114*, 7825.

(3) Dervan, P. B. (1992) *Nature 359*, 87.

(4) Sigman, D. S., Mazumder, A., and Perrin, D. M. (1993) *Chem. Rev. 93*, 2295.

(5) Sardesai, N. Y., Zimmermann, K., and Barton, J. K. (1994) *J. Am. Chem. Soc. 116*, 7502.

(6) Pratviel, G., Bernadou, J., and Meunier, B. (1995) *Angew. Chem., Int. Ed. Engl. 34*, 746.

(7) Keck, M.-V., and Lippard, S. J. (1992) *J. Am. Chem. Soc. 114*, 3386.

(8) Burrows, C. J., and Rokita, S. E. (1994) *Acc. Chem. Res. 27*, 295.

(9) (a) Breslin, D. T., and Schuster, G. B. (1996) *J. Am. Chem. Soc. 118*, 2311. (b) Breiner, K. M., Daugherty, M. A., Das, T. G., and Thorp, H. H. (1995) *J. Am. Chem. Soc. 117*, 11673. (c) Croke, D. T., Perrouslt, L., Sari, M. A., Battionti, J. P., Mansuy, D., Helene, C., and Doon, T. L. (1993) *J. Photochem. Photobiol. 18*, 41. (d) Nielsen, P. E. (1990) *J. Mol. Recognit. 3*, 1. (e) Bhattacharya, S., and Mandal, S. S. (1996) *J. Chem. Soc., Chem. Commun.*, 1515.

(10) (a) Papavassiliou, A. G. (1995) *Biochem. J. 305*, 345. (b) Siltani, A., Long, E. C., Pyle, A. M., and Barton, J. K. (1992) *J. Am. Chem. Soc. 114*, 2303.

(11) (a) Guajardo, R. J., Hudson, S. E., Brown, S. J., and Mascharak, P. K. (1993) *J. Am. Chem. Soc. 115*, 7971. (b) Stubbe, J., and Kozarich, J. W. (1987) *Chem. Rev. 87*, 1107. (c) Uhlmann, E., and Reyman, A. (1990) *Chem. Rev. 90*, 543.

(12) Jaeger, J., Santalucia, J., and Tinoco, I. (1993) *Annu. Rev. Biochem. 62*, 255.

(13) Taylor, S. J., Schultz, P. G., and Dervan, P. B. (1984) *Tetrahedron 40*, 457.

(14) (a) Kasprazak, K. S. (1991) *Chem. Res. Toxicol. 4*, 604. (b) Tullius, T. D., Ed. (1989) *Metal−DNA Chemistry*, ACS Symposium Series 402, American Chemical Society, Washington, DC. (c) Vahter, M. E. (1988) in *Biological Monitoring of Toxic Metals* (Clarkson, T. W., Friberg, L., Nordberg, G. F., and Sanger, P. R., Eds.) pp 303−321, Plenum, New York. (d) Yamanaka, K., and Okada, S. (1994) *Environ. Health Perspect. 102* (Suppl. 3), 37.

(15) Sato, K., Chikira, M., Fujii, Y., and Komatsu, A. (1994) *J. Chem. Soc., Chem. Commun.*, 625.

(16) (a) Gravert, D. J., and Griffin, J. H. (1993) *J. Org. Chem. 58*, 820. (b) Gravert, D. J., and Griffin, J. H. (1996) *Inorg. Chem. 35*, 4837.

(17) (a) Woodson, S. A., Muller, J. G., Burrows, C. J., and Rokita, S. E. (1993) *Nucleic Acids Res. 21*, 5524. (b) Muller, J. G., Paikoff, S. J., Rokita, S. E., and Burrows, C. J. (1994) *J. Inorg. Biochem. 54*, 199. (c) Burrows, C. J., and Rokita, S. E. (1994) *Acc. Chem. Res. 27*, 295.

(18) Routier, S., Bernier, J.-L., Waring, M. J., Colson, P., Houssier, C., and Baily, C. (1996) *J. Org. Chem. 61*, 2326.

(19) (a) Mandal, S. S., Vinaykumar, N., Varshney, U., and Bhattacharya, S. (1996) *J. Inorg. Biochem. 63*, 265. (b) Bhattacharya, S., and Mandal, S. S. (1997) *Biochem. Biophys. Acta 1323*, 29. (c) Mandal, S. S., Renuka, K., Guru Row, T. N., and Bhattacharya, S. (1996) *J. Chem. Soc., Chem. Commun.* 2725.

(20) Rajaram, R., Balachandran, U. N., and Ramasami, T. (1994) *Biochem. Biophys. Res. Commun. 205*, 327.

(21) Muller, W., and Crothers, D. M. (1975) *Eur. J. Biochem. 54*, 267.

(22) Reichmann, Y., Rice, S. A., Thomas, C. A., and Doty, P. (1954) *J. Am. Chem. Soc. 76*, 3047.

(23) Maniatis, T., Fritsch, E. F., and Sambrook, S. (1982) *Molecular Cloning*, p 458, Cold Spring Harbor Laboratory Press, Plainview, NY.

(24) Busetto, C., Cariati, F., Fusi, A., Gullotti, M., Marazzoni, F., Pasini, A., Ugo, R., and Valenti, V. (1973) *J. Chem. Soc.*, 754.

(25) Pyle, A. M., Rehmann, J. P., Meshoyrer, R., Kumar, C. V., Turro, N. J., and Barton, J. K. (1989) *J. Am. Chem. Soc. 111*, 3051.

(26) Meehan, T., Gamper, H., and Becker, J. F. (1982) *J. Biol. Chem. 257*, 10479.

(27) Cory, M., McKee, D. D., Kagan, J., Henry, D. W., and Miller, J. A. (1985) *J. Am. Chem. Soc. 107*, 2528.
(28) Sasse-Dwight, S., and Gralla, J. D. (1988) *J. Mol. Biol. 202*, 107.
(29) Sheldon, R. A., and Kochi, J. K. (1981) *Metal-Catalyzed Oxidation of Organic Compounds*, Academic, New York.
(30) (a) Koola, J. D., and Kochi, J. K. (1987) *Inorg. Chem. 26*, 908. (b) Chen, D., and Martell, A. E. (1987) *Inorg. Chem. 26*, 1026. (c) Yoon, H., and Burrows, C. J. (1988) *J. Am. Chem. Soc. 110*, 4087.
(31) (a) Cheng, C.-C., Goll, J. G., Neyhart, G. A., Welch, T. W., Singh, P., and Thorp, H. H. (1995) *J. Am. Chem. Soc. 117*, 2970. (b) Groves, J. T., and Kady, I. O. (1993) *Inorg. Chem. 32*, 3868. (c) Pamatong, F. V., Detmer, C. A., III, and Bocarsly, J. R. (1996) *J. Am. Chem. Soc. 118*, 5339. (d) Keek, M. V., and Lippard, S. J. (1992) *J. Am. Chem. Soc. 114*, 3386. (e) Carter, M. T., Rodriguez, M., and Bard, A. J. (1989) *J. Am. Chem. Soc. 111*, 8901.
(32) Singleton, S. F., and Dervan, P. B. (1992) *Biochemistry 31*, 1099.
(33) Goldsby, K. A., Blaho, J. K., and Hoferkamp, L. A. (1989) *Polyhedron 8*, 113.
(34) Srinivasan, K., Michand, P., and Kochi, J. K. (1986) *J. Am. Chem. Soc. 108*, 2309.

BC970121X